



## ***DETECTING COASTAL FEATURE CHANGES IN MEKONG DELTA USING MULTI-TEMPORAL LANDSAT AND GOOGLE EARTH IMAGES***

*D. Hak<sup>1</sup>, K. Nadaoka<sup>1</sup>, A. Collin<sup>2</sup>*

*<sup>1</sup>Department of Mechanical and Environmental Informatics, Graduate School of Information Science and Engineering, Tokyo Institute of Technology, E-mail:hak.d.aa@m.titech.ac.jp*

*<sup>2</sup>Littoral Geomorphology & Environment, Ecole Pratique des Hautes Etudes, E-mail: antoine.collin@ephe.sorbonne.fr*

### **ABSTRACT**

Investigating coastal feature changes is a crucial task focusing on the identification of potential factors that trigger the degradation of the coastal ecosystem. However, in-situ field investigations can be costly, time-consuming and almost impossible for multi-decadal assessment. In this study, the evolution of coastal features (including shoreline patterns and coastal habitats) in Kien Giang province, the north-westernmost part of the Mekong Delta, was investigated using multi-temporal Landsat data and high resolution Google Earth Images (GEIs). The aims of this study are three-fold: (i) to delineate and detect the inter-decadal shoreline evolution based on Landsat data; (ii) to detect the coastal land cover changes using Landsat data and GEIs; (iii) to evaluate the anthropogenic pressures on the coastal ecosystem, particularly the mangrove ecosystem. The results of this study revealed that from 1989 to 2014, the shoreline pattern of the study area has greatly changed due to the erosion and accretion phenomena that were driven by intensive human activities along the coastline. The rate of the coastal erosion has continuously increased until the present day with dominant erosion zone shifted from north to south. On the other hand, the coastal land cover has significantly and constantly changed. The bare surface has remarkably decreased while the other land covers such as the urban area, vegetation cover and inland water surface have successively increased. This reflects the increasing trend of human activities in this coastal region. Moreover, the contrast variation pattern of the paddy area and inland water surface shows that the socio-economic situation in the study site has changed from rice oriented to aquaculture oriented, which took place in early 2000s. The extent of the mangrove forest has continuously declined from 1995 until now. The conversion of the adjacent coastal land cover was found to have potential negative impacts on the degradation of the mangrove area. Moreover, concentrated economic activities such as the intensive shrimp breeding and rice cultivation, industrial development and increasing number of human inhabitants also have resulted in severe damage to the mangrove ecosystem.

**Keywords:** Remote sensing, Coastal feature, Change detection, Impact assessment

### **1 INTRODUCTION**

Coastal regions commonly feature very rich ecosystems, ranging from coastal wetlands, estuaries and mangrove forests, which provide extensive services and economic value, marking them as attractive places for human inhabitants. Nevertheless, many pristine coastal zones around the world have been altered to fulfill the socio-economic desires of human beings (e.g. Nile and Mekong delta). Coastal vegetation such as the mangrove and other aquatic plants make an ideal habitat and present abundant food sources for aquatic lives (Nagelkerken et al., 2008; Manson et al., 2005). Yet, overexploitation of coastal ecosystem services to feed a continuously growing population has led to the widespread elimination of natural habitats including mangrove forests and other kinds of vegetation which are effective barriers for protecting the coastal region against natural phenomena such as tsunami, storm surges and high waves. These immediate human impacts in combination with chronic climate change events will result in serious and long-term destruction of the entire coastal ecosystem (Klema, 2011). Investigating coastal feature changes is therefore a crucial task identifying potential factors that trigger the degradation of the coastal ecosystem. However, in-situ field

investigations can be costly, time-consuming and almost impossible for a multi-decadal assessment. Remotely sensed data has been used to alternatively map the coastal land cover and often produce reliable results compared to the ground-survey method (Kirui et al., 2011). The freely available Landsat images are widely used to study the coastal environment including habitat mapping and coastline changes assessment (e.g. Rokni et al., 2014; Santos et al., 2014; Cardoso et al., 2013; Niya et al., 2013). Moreover, the availability of high resolution Google Earth images in recent years has significantly attracted researchers to explore their potential use either as reference information to improve image classification results or as input data set to produce high accuracy classification image for both large and small scale study sites. For instance, Gong et al. (2010) used Google Earth images (GEIs), containing only three bands (red, green and blue), and its relevant visualization tools to locate marshland for wetland mapping across the whole China. Hu et al. (2013) conducted a comparison study to assess the ability of premium GEIs for land cover mapping of a regional scale study site and found that the classified image produced from GEIs is comparative to that produced from the original QuickBird image. Similarly, a recent study done by Collin et al. (2014) investigated the potential of GEIs for bathymetry and coastal habitat mapping at a very fine spatial scale (i.e. 0.6 m). Interestingly, they found that the bathymetry map derived from GEIs and the original QuickBird imagery are comparable and in some cases GEIs can even produce better results.

In this study, the evolution of coastal features (including shoreline patterns and coastal habitats) in Kien Giang province, located in the north-westernmost part of the Mekong Delta, was investigated using multi-temporal Landsat data and high resolution GEIs. The aims of this study are three-fold: (i) to delineate and detect the inter-decadal shoreline evolution based on Landsat data; (ii) to detect the coastal land cover changes using Landsat data and GEIs; (iii) to evaluate the anthropogenic pressures on the coastal ecosystem, particularly the mangrove ecosystem.

## 2 MATERIALS AND METHODS

### 2.1 Study Area

This study was conducted in Kien Giang province, located in the north-westernmost part of the Mekong delta, with the center point situated at  $10^{\circ}4'20.89''$  and  $105^{\circ}1'29''$ . The study site lays on a 113 km coastal strip, which encompasses about 1780 km<sup>2</sup> of Kien Giang coastal zone (Fig. 1). The average elevation of this coastal region is relatively low, ranges between 0.2-0.5 m above the mean sea level. This area contains a thin green belt of mangrove forests and poorly constructed dykes at some locations along the shoreline (IUCN, 2013; Duke et al., 2010).

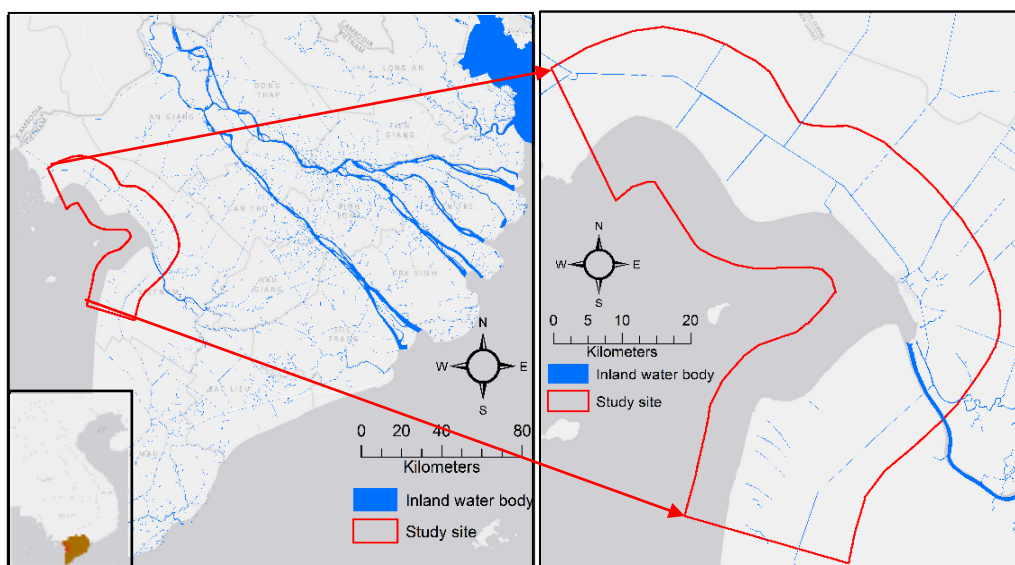


**Figure 1. Location map of the study area**

Areas of aquaculture, mixed rice-shrimp, paddy, sugarcane and other crops are found in the zone further inland. The low-lying topography compounded with a poor shoreline protective system makes this coastal region very vulnerable to the waves and tidal action, although the average wave height and tidal variation in this area are not so significant (the average wave height is about 0.3 m while the mean tidal range is approximately 0.56m). Being similar to the rest of the Mekong delta, the land cover condition of this area has remarkably changed over the two last decades due to the economic transition directed by the Vietnam government. Based on the records in Kien Giang province statistical year books, from 1996 to 2013 a large portion of its coastal land has been converted into shrimp fields, where the highest changes occurred between 2000 and 2004, from 34.6 thousands hectares to 79.2 thousands hectares (Fig. 6). The current socio-economic development of this area is significantly reliant on the agricultural sector (including crop cultivation, livestock, forestry, fishery and aquaculture production). In 2012, the economic share of this sector alone accounts for 40.02% of the total economic output of the whole province. However, this sector is considered vulnerable under the effect of climate change, especially in the face of the rising sea-level. A study conducted by the *Deutsche Gesellschaft für Internationale Zusammenarbeit* (GIZ) revealed that the shoreline erosion and accretion in this coastal zone were driven by a natural phenomenon due to the prevalence of the monsoon wind condition and wave height (GIZ, 2012). Between 2009 and 2010, about 30km of its total coastline underwent severe erosion. As consequences, coastal vegetation, fish ponds, dyke systems were significantly damaged and 19 coastal villages were directly affected (Duke et al., 2010). In addition to the impact of the natural events, anthropogenic activities, typically improper use of fertilizer, pesticide and overexploitation of groundwater, were also major factors which may trigger the coastal degradation of this area.

## 2.2 Methodology

The evolution of the shoreline and coastal land cover were investigated for the last two decades based on the analysis of a series of Landsat data and validated GEIs. To meet the objectives of this study multiple Landsat images including Landsat-7 ETM+, Landsat-5 and 4 TM were used. Moreover, two GEIs acquired on February 21, 2014 were used as the reference for both shoreline delineation and coastal land cover mapping (Fig. 2). The socio-economic information of year 1996 and 2000-2013 extracted from Kien Giang province statistical year books and Vietnam statistical year books were also used as ancillary information for assessing the impacts of

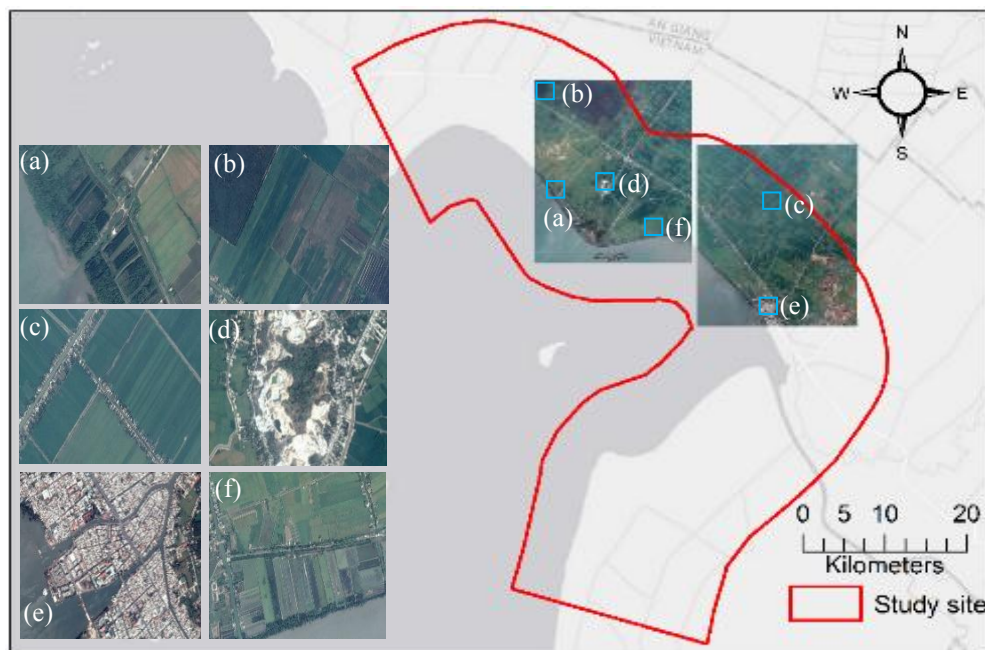


**Figure 2. Location map of the two Google Earth images used in this study and close-up visualization of the inherent primary habitats**

socio-economic activities on coastal habitats in the study area. The summary information of Landsat data set used in this study is given in Table 1. The detailed methodology for obtaining GEI is described in Collin et al. (2014).

**Table 1. Summary information of Landsat images used in this study**

Images source	Number of bands	Pixel size (m)	Date of acquisition
Landsat-7 ETM <sup>+</sup>	9	30 (MS) 15 (PAN)	21-02-2014
Landsat-7 ETM <sup>+</sup>	9	30 (MS) 15 (PAN)	13-02-2011
Landsat-7 ETM <sup>+</sup>	9	30 (MS) 15 (PAN)	07-02-2003
Landsat-7 ETM <sup>+</sup>	9	30 (MS) 15 (PAN)	22-04-2001
Landsat-5 TM	7	30 (MS)	09-02-1995
Landsat-4 TM	7	30 (MS)	05-04-1989
Landsat-4 TM	7	30 (MS)	31-01-1989

### 2.2.1. Shoreline and Coastal Land Cover Change Detection

The assessment of the shoreline pattern was carried out for the year 1989, 1995, 2001, 2003, 2011 and 2014 based on the analysis of 7 Landsat scenes (described in Table 1). In general, an image was used for delineating the shoreline position in one particular year. However, due to the presence of clouds that covered some portion of the coastline, two images were combined to generate the entire coastline for the year 1989. The basic technique of this integrated approach is straightforward. Firstly, the cloudy area of an image scene was masked by a simple masking technique. Later on, this masked area was replaced by a cloud free image from another Landsat scene by means of geo-referenced mosaicking. For a similar reason, land cover classification was carried out only for four periods including 1995, 2001, 2003 and 2014 due to the limitation of cloud free images over the study sites. To ensure the accuracy of classification, geometric and radiometric corrections were performed for all images prior to the image classification stage. Moreover, gap filling was applied on the images dated on 2003 and later, while cloud masking was performed on the 2001 and 2003 images to remove a very small portion (less than 1% of the study area) of cloudy area from images.

To investigate the spatio-temporal changes of the shoreline pattern, a single band threshold technique was firstly applied on each Landsat scene to create a binary image revealing the location of land and water boundary. Then, these land-water boundary images were vectorized and overlaid together for the further analysis. The spatio-temporal variation of the shoreline pattern, erosion and accretion rate were then identified based on the direct visualization and measurement of the shoreline position of these overlaid images. In this study, the threshold of  $b_5=550$  (surface reflectance value of the 5<sup>th</sup> band) was identified as the boundary between land and water area based on the direct visualization of each reflectance image.

Coastal habitat mapping were carried out using the maximum likelihood classifier, a supervised classification method, focused on eight major habitats including water surface, bare land, urban area, muddy, rocky and sandy, mangrove area, paddy area, inundated vegetation (indicated mangrove-shrimp or rice-shrimp area) and other vegetation area. By using GEIs as the ground truth dataset, 350 pixels were randomly selected from Landsat images for each type of habitat, from which 70% of these pixels were used as input points to train the maximum likelihood classifier site and 30% of these pixels were used for validating the classification results which were based on the confusion matrix technique. Selecting the training pixels is one of the most important steps in image classification, which can positively or negatively affect the classification results. A set of good training pixels should be pure enough to represent only one class and should be well distributed across the whole image in order to capture the maximum variation tied to a particular class. Yet, it is difficult to obtain these criteria, especially when the study area is characterized by highly heterogeneous habitats whose certain may appear as small patches amongst the other ones. To overcome this problem, the Isodata, an unsupervised classification method, was applied to all images prior to the selection of training pixels in order to identify the area where each class is concentrated. Then, the training pixels were randomly selected based on this unsupervised class image and labeled according to the reference GEI.

All the procedures of satellite image analysis in this study were carried out using the available tools in ENVI software version 5.0.

### 2.2.2. Assessment of Anthropogenic Impacts on Coastal Habitats

The impacts of the anthropogenic pressures on coastal habitat such as the mangrove area were identified by an exploratory statistical method, the Multiple Factor Analysis (hereinafter, MFA). Utilizing the MFA, the impacts of various socio-economic indicators on mangrove forests can be numerically and graphically interpreted. In this study, two groups of socio-economic indicators were employed as input data to the MFA in order to reveal the effects of human driven pressures on the extent of the mangrove area. The first group contains the information of eight land cover types extracted from the land cover mapping results for the year 1995, 2001, 2003 and 2014, plus the aquaculture breeding area obtained from the statistical year books of Vietnam and Kien Giang province. The second group comprises the information of population density and some economic outputs such as the production of aquaculture, production of paddy and gross output of industrial sector. For this latter dataset, the data associated with the year 1995 and 2001 were replaced by the data of year 1996 and 2000 respectively, due to the lack of information during that period. The MFA was carried out using XLSTAT, an add-in tool in Microsoft Excel.

## 3 RESULTS AND DISCUSSION

### 3.1. Variation of the Shoreline Pattern

The results of the shoreline pattern analysis revealed that from 1989 to the present day the coastline of the study area has substantially changed, both erosion and accretion were identified. In general, the erosion occurred in the northern and southern coast of the study site while the middle coastline was relatively stable, except for the coastal protrusion at the southern part where a significant accretion was manifested (Fig. 3). Moreover, the rates of erosion and accretion were spatially and temporally different. The average erosion rate from 1989 to 2014 was  $9.5 \text{ m} \cdot \text{year}^{-1}$  with an extreme erosion rate of  $44.5 \text{ m} \cdot \text{year}^{-1}$  appearing between 1989 and 1995 at the northern dominant erosion zone (zone (i) in Fig. 3). The annual erosion rates at zones (i) and (ii) in Fig. 3 during the period of 1995-2001, 2001-2003 and 2011-2014 were in the order of  $12.5 \text{ m} \cdot \text{year}^{-1}$ ,  $22.5 \text{ m} \cdot \text{year}^{-1}$  and  $28 \text{ m} \cdot \text{year}^{-1}$  respectively.

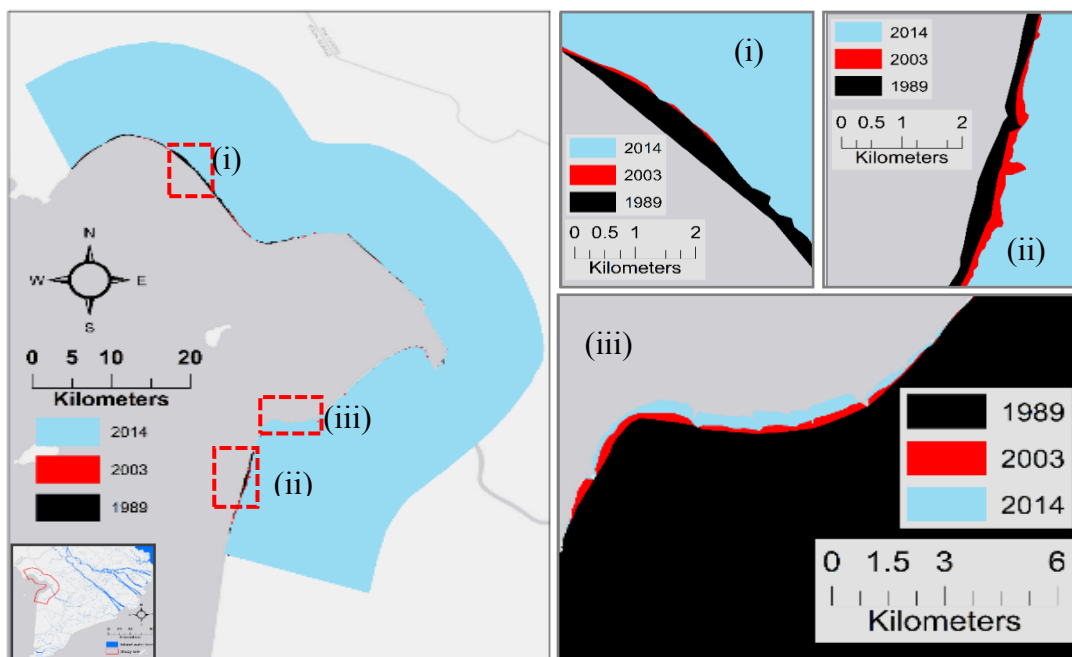


**Figure 3. Shoreline erosion and accretion pattern from 1989 to 2014: the dominant erosion zone (i and ii), and the accretion zone (iii)**

This increasing trend, especially the surge of erosion rate during 2001-2003, was more likely resulting from the rapid land cover conversion which occurred during that period due to the boom of aquaculture production (Fig. 6). Similarly to the variation of the erosion rate, the erosion pattern along the entire coastline was spatially distributed and temporally changed. From 1989 to 2014, the dominant erosion zone shifted from north to south. Remarkably, from 1989 to 2001, the coastal erosion was more prevalent at the northern part (Fig. 4 (a)), while from 2001 onward the most eroded part was found in the southern portion of the coastline (Fig. 4 (b)), adjacent to the area where the coastal land was rapidly invaded by shrimp breeding activities after the economic reform of Vietnam government in early 2000s. On the other hand, at the area where the accretion occurred (zone (iii) in Fig. 3), the average accretion rate between 1989 and 2014 was  $15.7 \text{ m}\cdot\text{year}^{-1}$  with the maximum rate of  $47.6 \text{ m}\cdot\text{year}^{-1}$ , was also found between 1989 and 1995. The accretion rate during the period of 1995-2001 and 2011-2014 were  $13 \text{ m}\cdot\text{year}^{-1}$  and  $11.5 \text{ m}\cdot\text{year}^{-1}$  respectively. There was no accretion occurring during 2000-2003; conversely, the abrupt increase in coastal erosion was found during this period. It is important to notice that the accretion area located just in the vicinity of the southern dominant erosion zone (Fig. 3) and is also bordering the area where the coastal land cover was severely altered by aquaculture activities. This can be inferred that land cover conversions into aquaculture farms during year 2000-2003 had tremendous adverse effects on the coastal erosion in this study site.

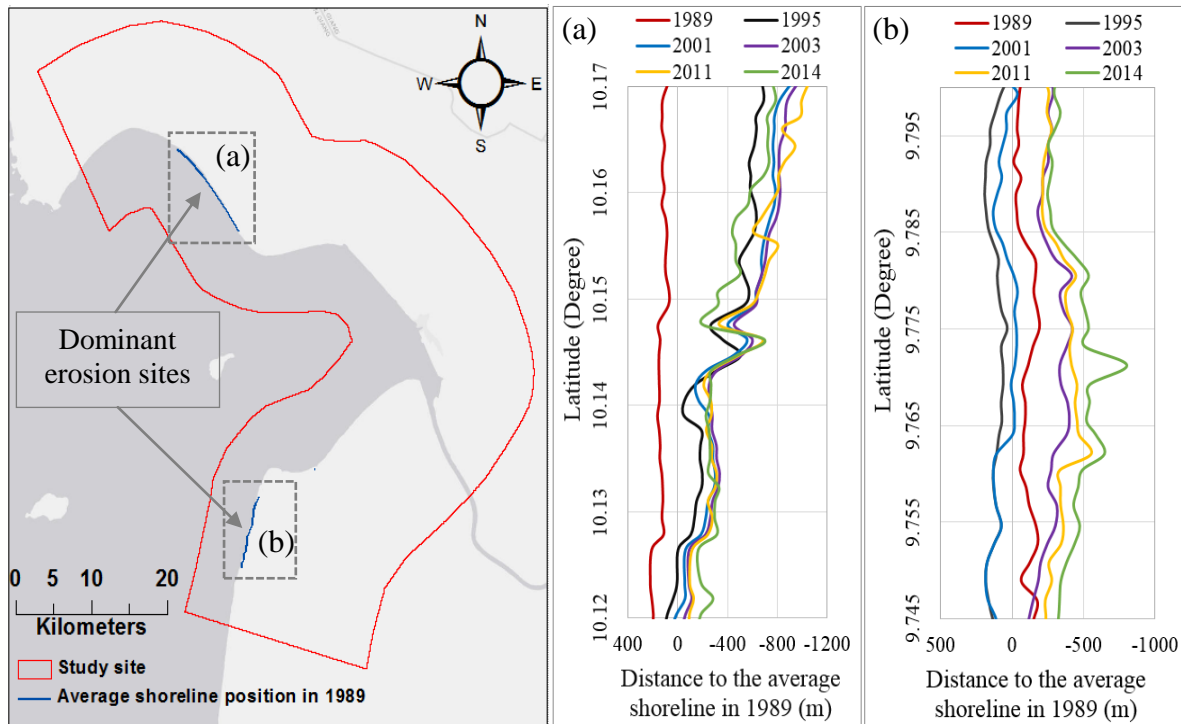


**Figure 4. Shoreline pattern variation from 1989 to 2014 at the most dominant erosion sites (negative value indicates erosion): shoreline position at the northern dominant erosion site (a); shoreline position at the southern dominant erosion site (b)**

Furthermore, according to the results of the study conducted by Duke et al. (2010), the erosion rate in some areas along KienGiang coastline can reach  $24 \text{ m}\cdot\text{year}^{-1}$  during 2009-2010. This finding combined with the results of our current study may be evidence showing that the shoreline erosion in KienGiang province is severe and constantly worsens. Moreover, although the erosion phenomenon in this area is considered as a natural event (GIZ, 2012), its increasing intensity is driven by the anthropogenic pressures, in particular, the massive changes of the coastal land use which occurred between the year 2000 and 2003. Furthermore, these human impacts remain unchanged until now regardless the presence of some coastal protection programs, which have been conducted in recent years (e.g. construction of sea dyke, artificial protecting fence and replanting of mangrove forest under GTZ KienGiang Biosphere Reserve Project).

### 3.2. Coastal Land Cover Changes

By using a representative training dataset, the maximum likelihood classifier provides satisfactory classification results. The overall classification accuracy and Kappa coefficient are 86.67% and 0.85, 81.87% and 0.79, 93.65% and 0.92, and 90.33% and 0.89 for the case of 2014, 2003, 2001 and 1995 respectively. The classified maps are given in Figure 5. Based on these classification results, the land cover in the study area has changed significantly from 1995 to 2014. Table 2 provides a summary of these results. In 1995, the vegetation (vegetation other than paddy and mangrove), bare land and paddy area were found to be the major land cover in the study site, whereas in 2014 paddy field became the most dominant land use, followed by other vegetation, inland water surface and other land cover types. The bare land area account for 34.17% of the total land area in 1995 and successively declined to 7.28% in 2014. For all cases, the bare land area was not prevalent in the middle part of the study site where most of the land area covered by paddy field, except the case of 2001 (Fig. 5).

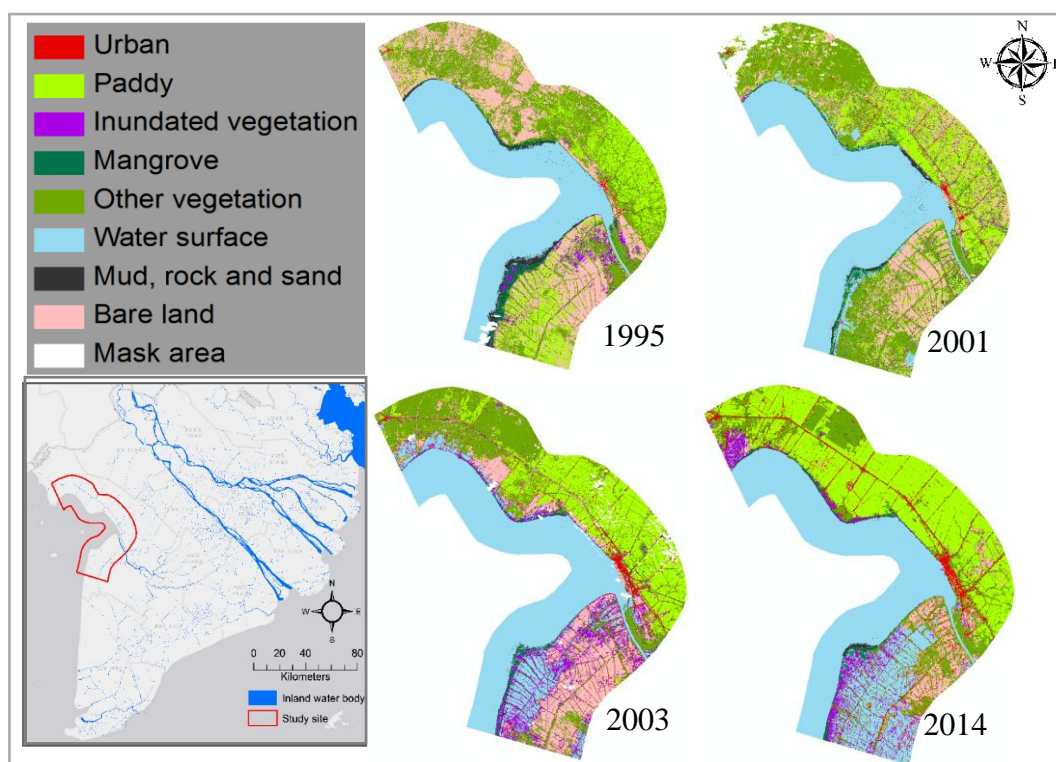


**Figure 5. Classification results of the coastal land cover of the study site in 1995, 2001, 2003 and 2014**

This exceptional case can be explained by the inconsistent acquisition date of input Landsat images used in this study (see Table 1). Regarding 1995, 2003 and 2014, the selected images were acquired during early to mid-February, which is the first half of the dry season.

**Table 2. Percentage of each land cover type compared with the total area of the study site in 1995, 2001, 2003 and 2014**

Land Cover	1995	2001	2003	2014
Urban	0.74%	1.41%	4.22%	6.35%
Paddy	18.84%	28.68%	25.21%	41.00%
Mangrove	3.61%	3.13%	2.43%	2.05%
Inundated vegetation	2.42%	5.26%	9.63%	6.07%
Other vegetation	37.20%	38.02%	27.40%	21.14%
Inland water	0.32%	3.68%	9.14%	14.84%
Mud, rock and sand	2.69%	1.48%	2.29%	1.27%
Bare land	34.17%	18.34%	19.67%	7.28%

Yet, in the case of year 2001, the input image was acquired in late April, the end of the dry season where most crops (paddy) may have been already harvested and the soil dryness has become more pronounced. The paddy area increased from 18.84 % in 1995 to 28.68 % in 2001 then dropped to 25.21 % in 2003 and peaked again at 41% in 2014. Similar to the variation trend of the paddy area, the area of inland water surface and inundated vegetation, which are more or less associated with aquaculture production, increased significantly between 1995 and 2014. The area of inland water surface increased from 0.32% in 1995 to 14.84 % in 2014 while the inundated vegetation area increased from 2.42 % in 1995 to 6.07 % in 2014. More interestingly, the variation trend of the inland water surface appeared as a quick jump between 2001 and 2003 (from 3.68% to 9.14%), indicating that the rapid land cover conversion into aquaculture pond in this study site happened during this period. These results concur very well with the variation trend of the aquaculture production area retrieved from the statistical year books of Kien Giang province (Fig. 6). On the other hand, during this period the paddy area has remarkably dropped. This can be explained by the socio-economic activities which have changed from rice oriented to aquaculture oriented between 2001 and 2003.

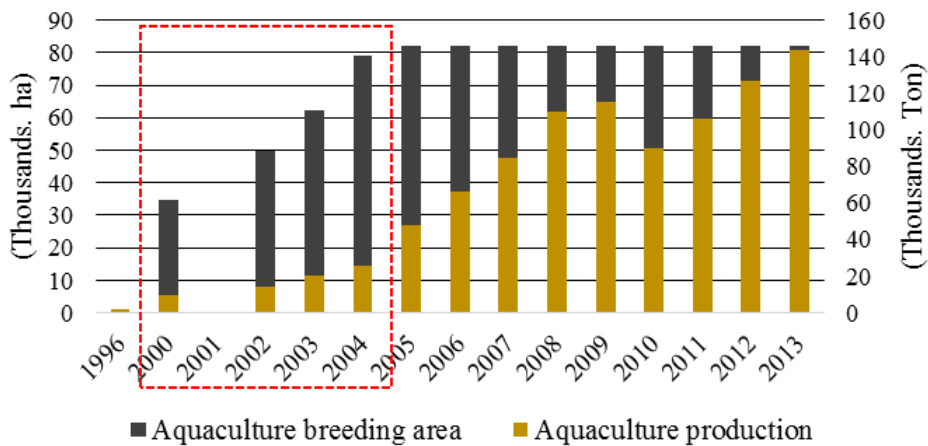


**Figure 6. Change in aquaculture breeding area and production in Kien Giang province from 1996 to 2013**

The mangrove area significantly declined from 1995 to 2014. It accounted for 3.61 % of the total land area in 1995 and dropped to 3.13 % in 2001, 2.43 % in 2003 and 2.05 % in 2014. In general, the average rate of mangrove loss between 1995 and 2014 was about 2.29 % of the total mangrove area per year. This declining rate is relatively high, and can lead to complete elimination of the mangrove forests from the coastline of the study area within 25 years if this decreasing trend persists.

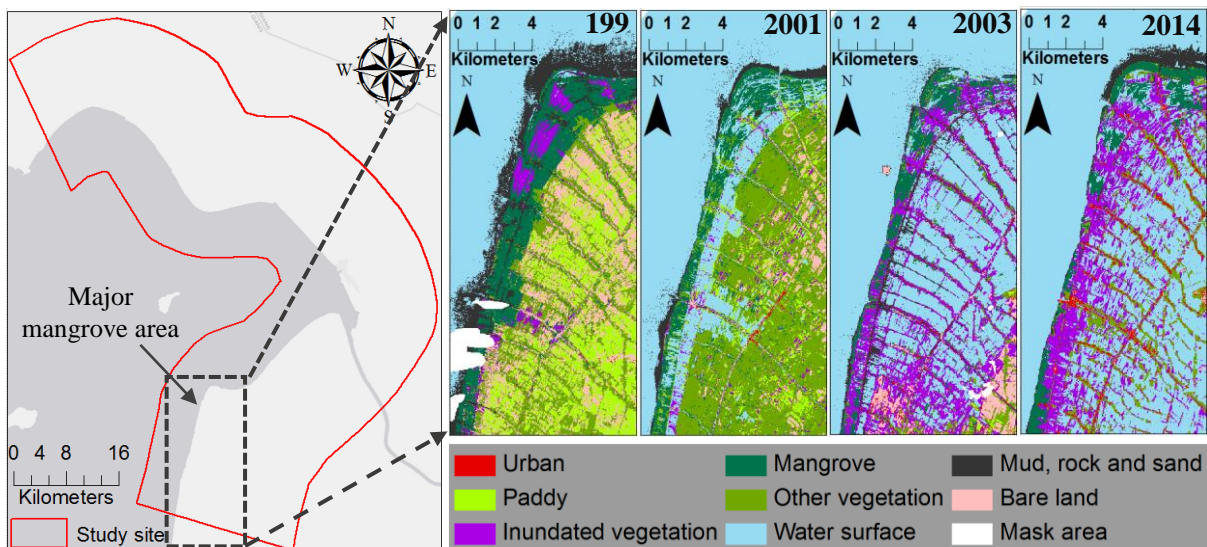


**Figure 7. Change in mangrove area and adjacent land use from 1995 to 2014 in the mangrove dominated zone**



This successive loss of the mangrove area were mainly resulting from the conversion of land use along the coastline which can be seen clearly in figure 7. Moreover, between 2001 and 2003 the rate of mangrove loss was as high as 11.16% of the total mangrove area per year. This rapid loss of the mangrove forest occurred coincidentally with the rapid increase of inland water surface and aquaculture area (Fig. 6) indicating the direct impact of aquaculture development on the degradation of the mangrove forest in this coastal zone. Aside from these human impacts, the natural even such as severe coastal erosion may also further trigger a destruction episode of the mangrove forests along the shoreline. As identified in this study, the area of mud, rock and sand, generally appearing in adjacent with the mangrove dominated zone (Fig. 5 and 7), has a similar variation trend to that of the mangrove extent, which successively and significantly declined from 1995 onward. It was about 2.69 % of the total land area in 1995 and dropped to 1.27 % in 2014. This similarity in the variation pattern clearly indicated that either the degradation of mangrove area triggered the coastal erosion episode or vice versa.

### 3.3. Anthropogenic Impacts on Coastal Habitats

The Fig.8 is the biplot graph of multiple factor analysis results, which depict the relationship between the variation of the mangrove area and some major economic indicators. It displays synoptically all variables and their corresponding factor loading (correlation of a variable with a factor). The first two factors (F1 and F2) accounted for 93.36% of the total data variability. Highly correlated variables would appear close to each other, meaning that they have a similar correlation level with the same factor.

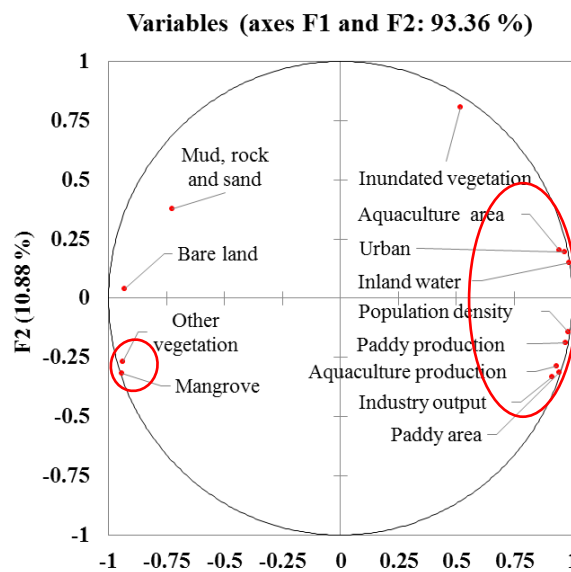


**Figure 8. Biplot graph showing the relationship between the mangrove area and major socio-economic indicators**

According to the results in Fig. 8, it is obvious that the mangrove area is strongly and negatively correlated with other types of land cover including urban area, inland water surface, aquaculture area, inundated vegetation and paddy area. The correlation coefficient between the mangrove area and above land cover types are -0.95, -0.97, -0.92, -0.77 and -0.82 with the  $p=0.05$  significant level, respectively. Likewise, the others socio-economic indicators such as the population density, the paddy production, the aquaculture production and the gross output of industrial sector were also negatively and significantly correlated with the extent of the mangrove area with the correlation coefficient of -0.89, -0.84, -0.79 and -0.72 respectively, all with the  $p=0.05$  significant level. Based on these results, the increase of inland water surface (most likely due to the increase of aquaculture breeding area) was the main driver leading to mangrove ecosystem degradation in this study site. The others major drivers were urban area, aquaculture area, population density, paddy production and paddy area. Interestingly, the paddy area seemed to have less adverse effects on the extent of the mangrove area compare to

the paddy production. This indicates that agricultural activities may indirectly affect the mangrove ecosystem with the most destructive effects stemming from the increasing amount of pollution load due to intensive agriculture practices. In contrast, the aquaculture area had a more pronounced effect on the reduction of mangrove area compared to the aquaculture production, revealing the direct impacts of land reclamation for aquaculture activities on the degradation of the mangrove forest along the coastline of this study area.

Based on the above results, it can be concluded that the land cover conversion due to socio-economic activities have remarkably triggered the decline of the mangrove cover in the study area. Furthermore, intensive activities tended to increase the production rate such as the aquaculture and paddy production combined with an increasing number of human inhabitants can further exacerbate the impacts.

#### **4 CONCLUSIONS**

From 1989 to 2014, the shoreline pattern of the study area has greatly changed due to the erosion and accretion phenomena which were intensified by concentrated human activities along the coastline, especially the conversion of the coastal land into aquaculture ponds between 2000 and 2003. The rate of the coastal erosion has continuously increased until the present day with the dominant erosion zone shifted from north to south. On the other hand, the coastal land cover has significantly changed across the time. The bare surface has remarkably decreased while the other land cover such as the urban area, vegetation cover and inland water surface have successively increased. This finding reflects the increasing trend of human activities in this coastal region. Moreover, the contrast variation pattern of the paddy area and inland water surface shows that the socio-economic situation in the study site has changed from rice oriented to aquaculture oriented especially in early 2000s. The extent of the mangrove forest has continuously declined from 1995 until now. The conversion of the coastal land cover due to the socio-economic development activities of the area was found to have potential negative impacts on the degradation of the mangrove area. Moreover, concentrated economic activities such as intensive shrimp breeding and rice cultivation, industrial development and increasing number of human inhabitants can result in more severe damages to the mangrove ecosystem. Although some programs aiming to protect the mangrove forests have been conducted in this coastal zone, they seem to be not effective enough to prevent the degradation of the inherent mangrove ecosystem.

#### **ACKNOWLEDGMENTS**

This study was supported by the ASEAN University Network of Southeast Asia Engineering Education Development Network Project (AUN/SEED-Net)-JICA program and Japan Society for Promotion of Science (JSPS) Core-to-Core Program (B. Asia-Africa Science Platforms), Grant-in-Aid for JSPS Fellows (No. 2402800), and Grant-in-Aid for Scientific Research (A) (No. 24246086 and 25257305) of JSPS.

#### **REFERENCES**

- Alongi, D. M. (2008) Mangrove forests: Resilience, protection from tsunamis, and responses to global climate change. *Estuarine, Coastal and Shelf Science*, 76(1), pp. 1–13. doi:10.1016/j.ecss.2007.08.024
- Cardoso, F.G., Jr, S.C. & Souza-Filho, M.W.P. (2013) Using spectral analysis of Landsat-5 TM images to map coastal wetlands in the Amazon River mouth, Brazil. *Wetland Ecology and Management*, 22 (1), pp.79-92. Doi:10.1007/s11273-013-9324-4
- Collin, A., Nadaoka, K., & Nakamura, T. (2014) Mapping VHR Water Depth, Seabed and Land Cover Using Google Earth Data. *ISPRS International Journal of Geo-Information*, 3(4), pp.1157–1179. doi:10.3390/ijgi3041157

Duke, N., Wilson, N., Mackenzie, J., Nguyen, H. H. & Puller, D. (2010). Assessing Mangrove Forests, Shoreline Condition and Feasibility of REDD for KienGiang Province Vietnam. GTZ KienGiang Biosphere Reserve Project, Technical Report

GIZ (2012) Coastal Rehabilitation and Mangrove Restoration using Melaleuca Fences, Practical Experience from KienGiang Province. GTZ KienGiang Biosphere Reserve Project, Technical report

Gong, P., Niu, Z., Cheng, X., Zhao, K., Zhou, D., Guo, J., Liang, L., Wang, X., Li, D., Huang, H., Wang, Y., Wang, K., Li, W., Wang X., Ying, Q., Yang, Z. Z., Ye, Y., Li, Z., Zhuang, D., Chi, Y., Zhou, H. & Yan, J. (2010) China's wetland change (1990–2000) determined by remote sensing. *Science China Earth Science*, 53 (7), pp.1036–1042. doi:10.1007/s11430-010-4002-3

Hu, Q., Wu, W., Xia, T., Yu, Q., Yang, P., Li, Z., Song, Q. (2013) Exploring the use of Google Earth imagery and object-based methods in land use/cover mapping. *Remote Sensing*, 5, pp.6026–6042. doi:10.3390/rs5116026

IUCN. (2013). Building Resilience to Climate Change Impacts: Coastal Southeast Asia KienGiang Province, Viet Nam. Factsheet.

Kirui, K. B., Kairo, J. G., Bosire, J., Viergever, K. M., Rudra, S., Huxham, M., & Briers, R. a. (2013) Mapping of mangrove forest land cover change along the Kenya coastline using Landsat imagery. *Ocean & Coastal Management*, 83, pp.19–24. doi:10.1016/j.ocecoaman.2011.12.004

Klemas, V. (2011) Remote sensing techniques for studying coastal ecosystems: an overview. *Coastal Research*, 27(1), pp.2-17. West Palm Beach (Florida)

Lee, T.-M., & Yeh, H.-C. (2009) Applying remote sensing techniques to monitor shifting wetland vegetation: A case study of Danshui River estuary mangrove communities, Taiwan. *Ecological Engineering*, 35(4), 487–496. doi:10.1016/j.ecoleng.2008.01.007

Manson, F.J., Loneragan, N.R., Skilleter, G.A. & Phinn, S.R. (2005) An evaluation of the evidence for linkages between mangroves and fisheries: a synthesis of the literature and identification of research directions. *Oceanography and Marine Biology-An Annual Review*, 43, pp. 483-513, ISSN 0078-3218

Nagelkerken, I., Blaber, S. J. M., Bouillon, S., Green, P., Haywood, M., Kirton, L. G., & Somerfield, P. J. (2008) The habitat function of mangroves for terrestrial and marine fauna: A review. *Aquatic Botany*, 89(2), 155–185. doi:10.1016/j.aquabot.2007.12.007

Niya, K.A., Alesheikh, A.A., Soltanpor, M. & Kheirkhahzarkesh, M.M. (2013) Shoreline change mapping using remote sensing and GIS. *Remote Sensing Applications*, 3(3).

Rokni, K., Ahmad, A., Selamat, A. & Hazini, S. (2014) Water feature extraction and change detection using multitemporal Landsat imagery. *Remote Sensing*, 6, 4173-4189, doi: 10.3390/rs6054173, ISSN 2072-4292

Santos, L. C. M., Matos, H. R., Schaeffer-Novelli, Y., Cunha-Lignon, M., Bitencourt, M. D., Koedam, N., & Dahdouh-Guebas, F. (2014) Anthropogenic activities on mangrove areas (São Francisco River Estuary, Brazil Northeast): A GIS-based analysis of CBERS and SPOT images to aid in local management. *Ocean & Coastal Management*, 89, 39–50. doi:10.1016/j.ocecoaman.2013.12.010